Journal of Molecular Liquids 359 (2022) 119219

Contents lists available at ScienceDirect

Journal of Molecular Liquids

journal homepage: www.elsevier.com/locate/molliq

Study of the ionic liquids' electrochemical reduction using experimental and computational methods

Sulafa Abdalmageed Saadaldeen Mohammed [a], Wan Zaireen Nisa Yahya [a,b,*], Mohamad Azmi Bustam [a,b], Md Golam Kibria [c], Asiah Nusaibah Masri [d], Nurul Diyana Mohd Kamonwel [a]

[a] Chemical Engineering Department, Universiti Teknologi PETRONAS, 32610 Seri Iskandar, Perak, Malaysia
[b] Centre for Research in Ionic Liquid, Universiti Teknologi PETRONAS, 32610 Seri Iskandar, Perak, Malaysia
[c] Chemical and Petroleum Engineering, University of Calgary, 2500 University Drive, NW, Calgary, Alberta T2N 1N4, Canada
[d] Energy Engineering Department, School of Chemical and Energy Engineering, Faculty of Engineering, Universiti Teknologi Malaysia, 81310 Skudai, Johor, Malaysia

ARTICLE INFO

Article history:
Received 4 February 2022
Revised 16 April 2022
Accepted 20 April 2022
Available online 26 April 2022

Keywords:
Ionic liquids
Electrochemical reduction
Stability
COSMO-RS

ABSTRACT

Ionic liquids (ILs) as electrolytes have attracted attention because of their distinctive properties. Numerous studies on the electrochemical stability of the ILs have been published. However, a deep understanding of the parameters that affect the reduction stability is highly required. In this study, the reduction potentials of five ILs including two novel ILs that contain 1,2,4-triazolium as cation were evaluated experimentally using cyclic voltammetry (CV) and compared with computational modeling using Tmolex software and Conductor like Screening Model for Real Solvents (COSMO-RS). We investigate the parameters that affect the ILs' reduction stability such as the lowest unoccupied molecular orbital (LUMO) energy levels of the cations and anions, as well as the effect of the molecular interaction between them. We conclude that while using the computational method, the individual values of the LUMO of the cations or anions without taking into consideration the molecular interaction might misguide the prediction of the ILs reduction stability.

1. Introduction

Ionic liquids (ILs) are a class of salt composed of ions that are in a liquid state below 100 °C. This particular property has made them largely used as solvent or electrolyte in various applications. Notably, the use of ILs in electrochemistry continues to increase due to their unique properties, such as in battery systems [1–5], dye-sensitized solar cells [6–10], CO_2 electrochemical reduction [11–14], and electrochemical capacitors [15–18]. In this context, numerous research papers have been published on the stability of ILs in terms of thermal, chemical, and electrochemical. Undeniably the understanding of the parameters that affect stability is highly required.

Generally, the electrochemical stability window of the electrolyte is described as the difference between the reduction and oxidation potentials of the electrolyte. On the other hand, the highest occupied molecular orbital (HOMO) and lowest unoccupied molecular orbital (LUMO) energy levels can be estimated using experimental oxidation and reduction peaks through Equations (1) and (2), respectively [19]:

$$E_{HOMO} = -(E_{(ox)onset} + 4.4)eV \quad (1)$$

$$E_{LUMO} = -(E_{(red)onset} + 4.4)eV \quad (2)$$

where E_{HOMO} and E_{LUMO} represent the energy levels of HOMO and LUMO in eV, $E_{ox(onset)}$ and $E_{red(onset)}$ correspond to the onset oxidation potential and the onset reduction potential, respectively. 4.4 is the reference energy level of ferrocene (4.4 eV under the vacuum level), versus saturated calomel (SCE) reference electrode.

Various studies were carried out to determine the ionic liquids' electrochemical stability window [20–24] through experimental and theoretical methods [25–29]. However, in the literature, the experimental individual oxidation and reduction potentials of the constituent ions have not been reported. From the experimental point of view, the reduction potential corresponds to the loss of

Abbreviations: HOMO, Highest occupied molecular orbital; LUMO, Lowest unoccupied molecular orbital; COSMO-RS, Conductor like Screening Model for Real Solvents.

* Corresponding author at: Chemical Engineering Department, Universiti Teknologi PETRONAS, 32610 Seri Iskandar, Perak, Malaysia.

E-mail addresses: sulafa_19001261@utp.edu.my (S. Abdalmageed Saadaldeen Mohammed), zaireen.yahya@utp.edu.my (W.Z.N. Yahya), azmibustam@utp.edu.my (M.A. Bustam), md.kibria@ucalgary.ca (M.G. Kibria), nusaibah@utm.my (A.N. Masri), nurul.diyana_24411@utp.edu.my (N.D. Mohd Kamonwel).

https://doi.org/10.1016/j.molliq.2022.119219
0167-7322/

electrons based on the total interaction of both cations and anions in the electrolyte solution. Meanwhile, from the theoretical point of view, the cathodic and anodic potential limits were estimated from the quantum chemical calculation of the highest occupied molecular orbital (HOMO) and the lowest unoccupied molecular orbital (LUMO) energies of individual cations and anions. In this case, it is assumed that the cathodic limit (reduction potential) of the majority of the ionic liquids is determined by the cation's reduction potential, while the oxidation of the anion is determined by the anodic limit (oxidation potential) [30–32]. However, this statement may not always be true according to theoretical and experimental studies [33].

For example, the computational study conducted by Ong and Andreussi [23] and the experimental study by Howlett [34] displayed that the broadly used bis(trifluoromethylsulfonyl)imide (TFSI) anion reduces more easily than the *N*-propyl-*N*-methylpyrrolidinium cation. It was reported that for the electrolyte to be thermodynamically stable, the electrode electrochemical potentials $\mu_{cathode}$ (cathode Fermi energy) and μ_{anode} (anode Fermi energy level) must be located within the HOMO and LUMO of the electrolyte [35]. However, recent studies showed that the actual position of the electrochemical window is observed to be located in the HOMO–LUMO energy gap, but not necessarily at the exact values of the HOMO and LUMO [35,36].

Li et al. investigated the electrochemical potential windows of 33 ILs experimentally, to study the effect of cation, anions, electrode material (working and reference) as well as the water content of the ionic liquids [37]. They reported that using glassy carbon (GC) as working electrode showed the largest potential window compared to gold (Au) and platinum (Pt) electrode, meanwhile, an increase in the water content narrows the electrochemical window for each ILs. They highlighted that the molecular interaction between the cation and anions plays significant role in determining the electrochemical potential windows (EPWs) of ILs besides the stability of cations and anions. Similarly Greaves and Asoka [38] suggested that the molecular interactions may consist of hydrogen bond interaction, hydrophilic interaction and ion-ion interaction.

Meanwhile, Xue and Qin [39] stated that the electrochemical window is specified by the cation as well as the anion. A less stable ion may have an impact on the stability through the interaction between the produced components from the decomposition with a more stable ion (opposite charge of the ion). We find that this viewpoint will enhance the selection process for the optimum IL for specific applications. For instance, in CO_2 electrochemical reduction, it has been reported that the activity of the ILs is due to the low LUMO value of the cation [40,41]. Hence, in this type of application, cations with low LUMO values are required while maintaining the electrochemical stability of the ILs.

In this work, computational and experimental methods are used to analyze the parameters affecting the reduction stability of ILs. The computational study was carried out using TmoleX and Conductor-like Screening Model for Realistic Solvents (COSMO-RS) software. TmoleX software allows users to run the entire workflow of a quantum chemical investigation in a user-friendly graphical front end, from the initial building of a structure to the visualization of the results [42]. In this study, TmoleX was used to calculate the LUMO values of different cations and anions. COSMO-RS software is a quantum chemical calculation tool to compute the chemical potential differences of molecules in liquids. The software developed by Klamt [43] has gained attention because of its ability to predict the thermodynamic properties and behavior of ionic liquids in a variety of applications [44–46]. In this study, COSMO-RS was used to calculate the molecular interaction energies for the selected ILs.

The experimental reduction potentials of five ILs composed of imidazolium-based ILs and triazolium-based ILs as shown in Fig. 1 were determined via cyclic voltammetry. Commercially

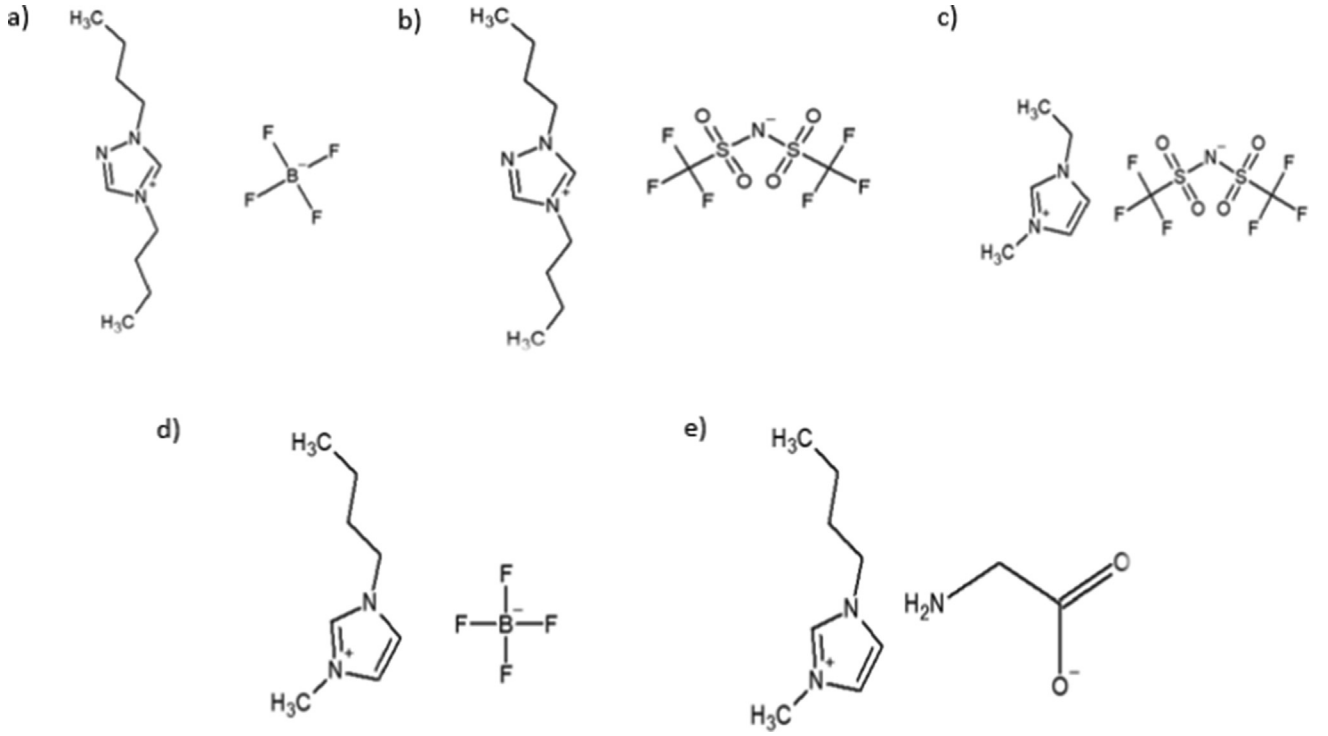

Fig. 1. Molecular structures of (a) 1,4-dibutyl-1,2,4-triazolium tetrafluoroborate (BBT BF_4), (b) 1,4-dibutyl-1,2,4-triazolium bis(trifluoromethylsulfonyl)imide (BBT TFSI), (c) 1-ethyl-3-methylimidazolium bis(trifluoromethylsulfonyl)imide (EMIM TFSI), (d) 1-butyl-3-methylimidazolium tetrafluoroborate (BMIM BF_4) and (e) 1-butyl-3-methylimidazolium glycine (BMIM Gly).

available 1-ethyl-3-methylimidazolium bis(trifluoromethylsulfonyl)imide (EMIM TFSI) was used and the remaining four ILs were synthesized. This study is aimed to provide a plausible explanation of how the LUMO values of the individual anions and cations, as well as their electrostatic interactions, could affect the reduction stability. This will optimize the usage of the computational method in predicting the electrochemical stability since ILs are considered as designer liquids and many combinations of cations and anions can be achieved, which makes the experimental study of electrochemical stability not efficient for the selection of huge sets of ILs.

2. Materials and methods

2.1. Materials

All starting materials and chemicals used are commercially available and used without further purification unless otherwise stated. 1,2,4-triazole (98 % purity), methanol, sodium tetrafluoroborate (98 % purity), acetone, ethyl acetate, lithium bis(trifluoromethanesulfonyl)imide (99.95 % purity) were procured from Sigma-Aldrich. 1-bromobutane (99 % purity), and sodium methoxide (pure, 5.4 M, 30 wt% solution in methanol) were procured from Acros Organic. 1-ethyl-3-methylimidazolium bis(trifluoromethylsulfonyl)imide (EMIM TFSI), chloroform, and acetonitrile were procured from Merck. Dichloromethane was procured from Fisher while glycine (99 % purity) was procured from Fluka Analytical.

2.2. Synthesis of the ILs

2.2.1. Synthesis of 1,4-dibutyl-1,2,4-triazolium bromide (BBT Br) ionic liquid

1,4-dibutyl-1,2,4-triazolium bromide (BBT Br) ionic liquid was synthesized through the combination and modification of the methods by Atkinson [47] and Belletire [48]. The proposed procedure avoids the limitations of both methods such as the extreme condition that affects the properties of the product in the first method as well as the product loss from successive extractions in the second method. The product loss is due to the product solubility in chloroform and partially soluble in water, while the reactants are highly soluble in water and partially soluble in chloroform. In this study, 3.0 g of 1,2,4-triazole (43.43 mmol) was added to 22.2 ml of methanol. Then, 7.8 g sodium methoxide (30 wt% in methanol, 43.43 mmol) was added dropwise to the solution in an ice bath. The reaction mixture was stirred for 10 min at room temperature until all the components were completely dissolved. Then, 6.67 g 1-bromobutane was added dropwise to the mixture in the ice bath. The ice bath was removed and replaced with an oil bath. After that, the reaction mixture was heated to 60 °C and stirred at 320 rpm under reflux for 24 h, then cooled to room temperature. The methanol was removed using a rotary evaporator resulting in a yellow oil. 40 ml of chloroform was added to the oil under reflux at 55 °C and continued to stir at 400 rpm for 24 h to extract the targeted product, followed by a cooling process at 5 °C to precipitate the non-reacted materials. Then, the mixture was filtered. The chloroform solvent was removed from the filtrate using a rotary evaporator, resulting in a yellow viscous liquid which is 1-butyl-1,2,4-triazole, (4.71 g, 88 % yield). ^{1}H NMR for 1-butyl-1,2,4-triazole: δ ppm ($CDCl_3$) 0.883 (t, 3H),1.275 (m, 2H), 1.805 (m, 2H), 4.104 (t, 2H), 7.868 (s, 1H) and 7.984 (s, 1H).

3.57 g of 1-bromobutane (26.05 mmol) was added dropwise to 2.51 g of 1-butyl-1,2,4-triazole (20.04 mmol) in an ice bath. The ice bath was then removed and replaced with an oil bath. The reaction mixture was heated at 80 °C and stirred at 320 rpm for 24 h under reflux and then cooled to room temperature, resulting in a brownish gel. 20 ml of ethyl acetate was added to the gel and the mixture was heated at 35 °C and stirred at 400 rpm for 3 min to melt the gel, resulting in two liquid layers, the top layer is the solvent while the ionic liquid was at the bottom layer. Then, the remaining solvent was removed from the bottom layer using a rotary evaporator, resulting in a brown gel product of 1,4-dibutyl-1,2,4-triazolium bromide (BBT Br) (4.7 g, 90 % yield) at room temperature. ^{1}H NMR for 1,4-dibutyl-1,2,4-triazolium bromide: δ ppm (D_2O) 0.866 (m, 6H), 1.286 (m, 4H), 1.853 (m, 4H), 4.263 (t, 2H), 4.363 (t, 2H), 8.831 (d, 1H), 9.799 (d, 1H).

2.2.2. Synthesis of 1,4-dibutyl-1,2,4-triazolium tetrafluoroborate (BBT BF_4)

7.01 g of sodium tetrafluoroborate ($NaBF_4$) was dissolved in 200 ml methanol. Then, 15 g of 1,4-dibutyl-1,2,4-triazolium bromide (BBT Br) was added to the solution. The mixture was stirred at 320 rpm for 48 h at 25 °C. After that, the methanol was removed, and 130 ml acetone was added, resulting in a solid particle which was separated through filtration process. Then, the solvent was removed using rotary evaporator. The mixture was washed again using 130 ml of dichloromethane to separate the remaining impurities. Solid particles were formed. The particles were removed through filtration process and the solvent was removed from the product using rotary evaporator. The resulting product is 1,4-dibutyl-1,2,4-triazol-4-ium tetrafluoroborate (BBT BF_4) (98 % yield).

2.2.3. Synthesis of 1,4-dibutyl-1H-1,2,4-triazol-4-ium bis (trifluoromethylsulfonyl)imide (BBT TFSI)

4.93 g of lithium bis(trifluoromethanesulfonyl)imide (LiTFSI) was dissolved in 18 ml water. Then, 3.78 g of 1,4-dibutyl-1,2,4-triazolium bromide (BBT Br) was added to the solution. Then, the mixture was stirred at 1000 rpm for 48 h, forming two layers. The brown bottom layer was separated from the mixture using a separating funnel and washed with 50 ml of water three times. Then, the water was removed using a rotary evaporator. The resulting product is 1,4-dibutyl-1,2,4-triazolium bis(trifluoromethylsulfonyl)imide (BBT TFSI), (67 % yield).

2.2.4. Synthesis of 1-butyl-3-methylimidazolium bromide (BMIM Br)

21.0 g of 1-bromobutane 99 % was added dropwise to 10.7 g of 1-methyl imidazole in the ice bath. Then, the mixture was heated at 70 °C and stirred at 320 rpm for 28 h under reflux. The mixture was then cooled to room temperature. 80 ml of ethyl acetate was added to the mixture and stirred at 400 rpm at 35 °C for 30 min to avoid the crystallization of reaction components at room temperature. The solvent was removed using a rotary evaporator, resulting in 1-butyl-3-methylimidazolium bromide (BMIM Br), (93 % yield) as a yellow viscous liquid. ^{1}H NMR for of 1-butyl-3-methylimidazolium bromide (BMIM Br) δ ppm (D_2O) 0.835 (t, 3H), 1.227 (m, 2H), 1.768(m, 2H), 3.813 (s, 3H), 4.119 (t, 2H), 7.353(d, 1H), 7.404(d, 1H), 8.646 (s, 1H).

2.2.5. Synthesis of 1-butyl-3-methylimidazolium tetrafluoroborate (BMIM BF_4)

8.26 g of sodium tetrafluoroborate (NaBF4) was dissolved in 250 ml of methanol, followed by the addition of 15.03 g of 1-butyl-3-methylimidazolium bromide (BMIM Br). The mixture was stirred at 320 rpm for 48 h at 25 °C. The methanol was removed using rotary evaporator. After that, 130 ml of dichloromethane was added to the mixture, resulting in a solid particle which was separated through filtration process. The washing process was repeated three times, until no more solid particles formation. The solvent was removed from the product using rotary evaporator. The resulting product is 1-butyl-3-methylimidazolium tetrafluoroborate (BMIM BF4), 77.04 % yield).

2.2.6. Synthesis of 1-butyl-3-methylimidazolium glycine (BMIM Gly)

10 g of (BMIM Br) was dissolved in 35 ml of water. The solution was then poured to 41 g of AMBERLITE IRA400CL OH- resin in the anion exchange column, resulting to 1-butyl-3-methylimidazolium hydroxide (BMIM OH) in water. The (BMIM OH) solution was mixed with glycine solution (2 M) at a 1:1.1 M ratio. The mixture was stirred at 500 rpm at room temperature for 12 h. Then, the water was removed using a rotary evaporator. After that, the mixture was mixed with a methanol/acetonitrile mixture (1:4 vol ratio). The precipitated glycine was then filtered out, and the washing process was repeated two times. Then, the solvents were removed using a rotary evaporator, resulting in a yellow liquid of 1-butyl-3-methylimidazolium glycine (BMIM Gly), (51.22 % yield). 1H NMR for of 1-butyl-3-methylimidazolium glycine δ ppm (DMSO) 0.890 (t, 3H), 1.244 (m, 2H), 1.777 (m, 2H), 2.788 (s, 2H), 3.918 (s, 3H), 4.234 (t,2H), 7.863 (d, 1H), 7.929 (d, 1H), 9.991 (s, 1H).

2.3. Structure confirmation of ionic liquids

2.3.1. Proton nuclear magnetic resonance (^{1}H NMR)

The structures of the synthesized ionic liquids were confirmed via proton nuclear magnetic resonance (1H NMR) using Bruker AVANCE III 500 MHz. Deuterated dimethylsulfoxide (DMSO) and deuterium oxide (D_2O) were used as solvents. The analysis was done using Topspin software.

2.3.2. Fourier transform infrared spectroscopy (FTIR)

Various functional groups were detected by Fourier transform infrared spectroscopy-attenuated total reflectance (FTIR-ATR) using ThermoNicolet iS5 by Thermo Fisher Scientific (Waltham, Massachusetts, USA) in the range of 4000 to 400 cm-1 under 64 scanning.

2.3.3. Ion chromatography (IC)

Ion chromatography (IC) was used to measure the concentrations of bromides anions. Na_2CO_3 (1 mmol/L) /$NaHCO_3$ (4 mmol/L) mixture was used as the eluent on Metrosep A Supp 4–250/4.0 column within an acceptable run-time (30 min) and 1.000 ml/min flow rate.

Procedures/Data: All other relevant characterization data, original spectra, etc., are provided in the Supporting Information.

2.4. Reduction peak measurement

In this study, the reduction peak for all selected ILs at the potential range of −2.5 to 0 V was measured via cyclic voltammetry (CV) using EIS510 multichannel EIS system (WonATech Co.ltd). The experiment was done at a 10 mV/s scan rate, and 5 A limiting current. Glassy carbon was used as the counter electrode, platinum wire as the working electrode, and saturated calomel electrode (SCE) as the reference electrode.

2.5. Evaluation of HOMO and LUMO values using TmoleX software

To extract the LUMO and HOMO values of the anions and cations of the ILs, Tmolex simulation software was employed based on the density functional theory (DFT) using triple-zeta valence with polarization (TZVP) parametrization.

2.6. Evaluation of molecular interaction using COSMO-RS software

In this study, COSMO-RS was used to predict the interaction energies of the different ILs. Along with the analysis, the COSMO-RS related theory and the corresponding importance of the simulated properties were already discussed by the developer [49,50].

3. Results and discussion

The reduction potentials of 1,4-dibutyl-1,2,4-triazolium tetrafluoroborate (BBT BF_4) and 1,4-dibutyl-1,2,4-triazolium bis(trifluoromethylsulfonyl)imide (BBT TFSI) were determined to study the effects of anions as shown in Fig. 2. On the other hand, the HOMO/LUMO values of the ILs calculated computationally are shown in Fig. 3. From Fig. 2, it can be observed that BBT TFSI is more stable in terms of reduction compared to BBT BF_4. The reduction potential was −1.65 V for BBT BF_4 and −1.93 V for BBT TFSI. These results suggest that BBT BF_4 has a lower LUMO value based on the calculation using Equation (2) of −2.75 eV versus −2.47 eV for BBT TFSI, as shown in Table 1. However, the computational calculation of HOMO/LUMO values shown in Fig. 3 depicts a conflicting result where the LUMO value for TFSI anion is significantly lower. Thus, the trend shown for the predicted LUMO anions values by computational method is not reliable to sufficiently draw a conclusion on the reduction stability.

Pekka and Hubert [36] developed thermodynamic model to estimate the electrochemical stability of the electrolyte, based on redox potentials and Fermi level of the electron inside the solution. They reported that the redox potentials are correlated to the difference in Gibbs free energy between the reactants and the product. While the redox potentials in some circumstances show strong correlation with HOMO energies. The deviation of the calculated energy levels was explained by the influence of electrolytes and other molecules in the system.

Hence, there could be another parameter affecting the stability of ILs, which is probably the molecular interaction as suggested by Xue [39] and Zhao [3]. Recent studies are carried out to investigate the effects of molecular interaction on ILs stability [51,52]. Muraledharan [51] reported that amino acid-based dicationic ionic liquids showed wider electrochemical window than monocationic ionic liquids due to the strong interaction and higher binding energy between cation–anion in the dicationic ionic liquids.

To provide further clarification on this hypothesis, COSMO-RS was used to study the molecular interaction energies (MIE). MIE mainly consist of hydrogen bond interaction (E_{HB}), electrostatic or misfit interaction (E_{misfit}), and van der Waals forces (E_{vdw}) [53,54]. The interaction energies generated by COSMO-RS are functions of the screening charges of two interacting surface segments σ, σ' or $\sigma_{acceptor}$, σ_{donor} as shown in the following equations [54]:

$$E_{misfit}(\sigma,\sigma') = a_{eff} * (a'/2) * (\sigma+\sigma')^2 \quad (3)$$

$$E_{HB} = a_{eff} C_{HB} \min(0; \min(0; \sigma_{donor} + \sigma_{HB}) \max(0; \sigma_{acceptor} - \sigma_{HB}) \quad (4)$$

$$E_{vdw} = a_{eff}(\tau_{vdw} + \tau'_{vdw}) \quad (5)$$

where a_{eff} is the effective contact area between two surface segments, σHB is the cutoff for hydrogen–bonding, α' is an interaction parameter; C_{HB} is the hydrogen–bond strength; τ_{vdw} and τ'_{vdw} are element-specific adjustable van der Waals interaction parameter.

The COSMO sigma surfaces for the selected cations and anions of the ILs is shown in Fig. 4 and the molecular interaction energy values are listed in Table 2. The sigma surface provides visualization of the charge distribution on the surface of the cation and anion respectively. The blue region shows an underlying positive charge brought by the hydrogen of the BBT and imidazolium rings, the green represents the neutralization nature, yellow part for partial electronegativity, while the red part represents a strong electronegativity. The result shows that the total interaction energies of BBT TFSI is higher than that in BBT BF_4 as shown in Table 2. It can be deduced that the strong attraction force between BBT and TFSI obstructs the flow of reduction's electrons toward the cation which enhances the stability. Moreover, the strong repulsion force

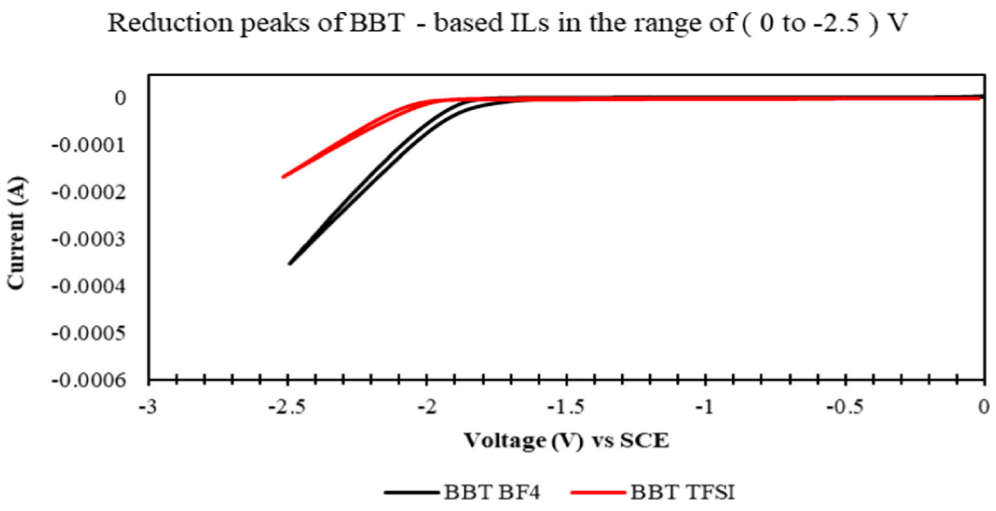

Fig. 2. Comparison of BBT BF_4 and BBT TFSI in terms of the reduction peaks.

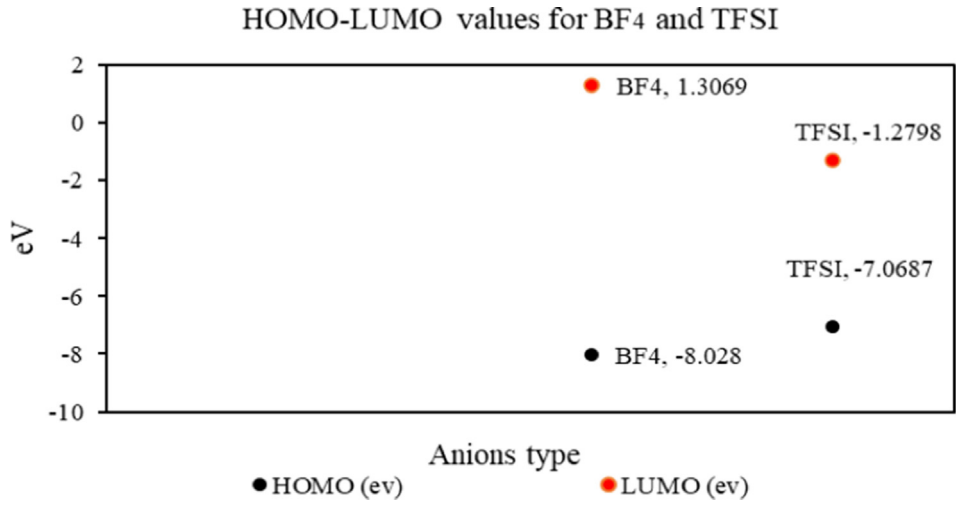

Fig. 3. HOMO-LUMO values for BF_4 and TFSI anions using Tmolex.

Table 1
Experimental reduction potential, calculated LUMO values and LUMO values from computational methods.

IL Name	Experimental Reduction peak (V)	Calculated LUMO value (eV) $E_{LUMO} = -(E_{red} + 4.4)$ eV	LUMO value for the cation (eV) using Tmolex	LUMO value for the anion (eV) using Tmolex
BBT BF_4	−1.65	−2.75	−2.3675	1.3069
BBT TFSI	−1.93	−2.47	−2.3675	−1.2798
BMIM Gly	−2.06	−2.34	−1.7779	0. 2353
BMIM BF_4	−1.70	−2.70	−1.7779	1.3069
EMIM TFSI	−2.22	−2.18	−1.7643	−1.2798

between TFSI anion (negative charge) and the reduction's electrons also enhance the stability. To further validate the assumption, the reduction potentials of 1-butyl-3-methylimidazolium tetrafluoroborate (BMIM BF_4) and 1-butyl-3-methylimidazolium glycine (BMIM Gly) were also compared as shown in Fig. 5. From Fig. 5, it can be observed that BMIM Gly is more stable compared to BMIM BF_4, where the reduction peak is −2.06 V for BMIM Gly while it is −1.70 V for BMIM BF_4, which indicates that BMIM BF_4 has a lower LUMO value. This is opposite to the results obtained from the computational prediction of LUMO energy levels as depicted in Fig. 6.

By analyzing Table 2 it can be observed that the total interaction energies of BMIM Gly are higher than BMIM BF_4, which is also consistent with the results obtained by TFSI anion. It can be noted that the effect of the anions on the electrochemical stability against reduction is mainly through molecular interaction energies since the anion is not highly affected by the reduction electron due to the repulsion force. However, these interaction energies affect the stability of IL since they affect the cations-anions interaction which impedes the reduction's electrons. Recent studies reported that although ILs have lower LUMO values when compared to organic solvents/electrolytes, they have strong resistance against

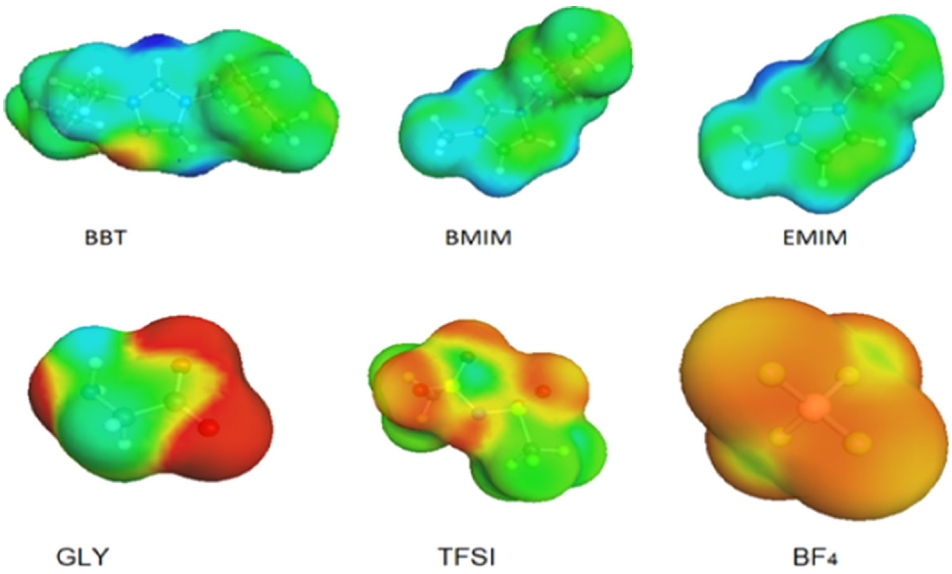

Fig. 4. Sigma surface for selected cations and anions using COSMO-RS. The colour is used to determine the charge distribution of the molecule, accordingly; green colour represents the neutral nature, red colour represents the strong electronegativity, yellow colour represents a partial negative charge, and the blue colour represents a positive charge area. (For interpretation of the references to colour in this figure legend, the reader is referred to the web version of this article.)

Table 2
Misfit (H_MF) energies, hydrogen bond interaction (H_HB), van der Waals forces (H_vdw), and total interaction energies in kcal.mol-1 generated by COSMO-RS.

IL Name	H_MF (kcal.mol^{-1})	H_HB (kcal.mol^{-1})	H_vdw (kcal.mol^{-1})	Total interaction energies (kcal.mol^{-1})
BBT BF_4	7.4	−3.271	−14.438	−10.309
BBT TFSI	7.777	−1.348	−18.623	−12.194
BMIM Gly	12.78	−9.709	−14.276	−11.205
BMIM BF_4	6.805	−2.836	−12.165	−8.196
EMIM TFSI	6.426	−1.098	−14.643	−9.315

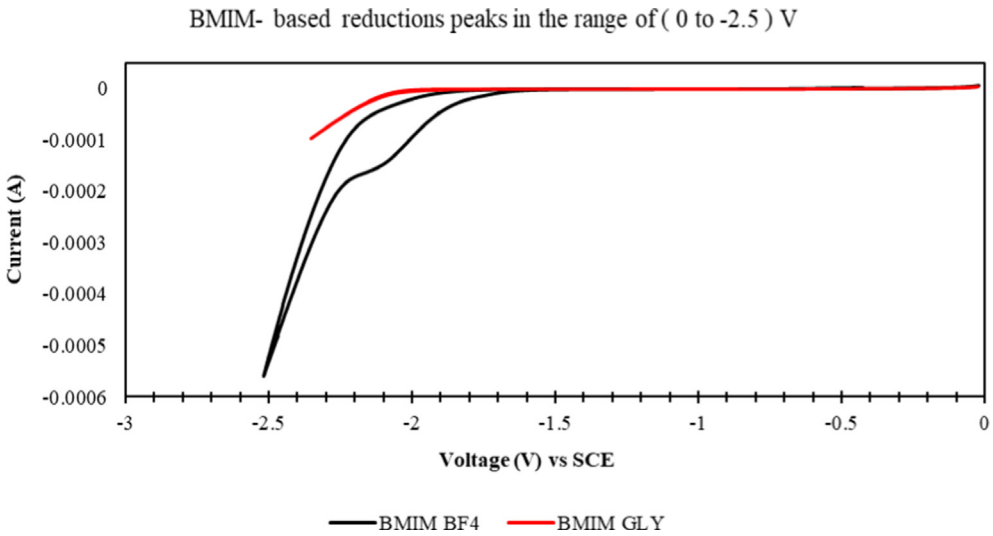

Fig. 5. Comparison between (BMIM BF_4) and (BMIM Gly) in term of reduction peaks.

the reduction, and this is due to their capability to produce better film formation at higher potential due to molecular interaction [55,56]. It can be noted that for ILs having similar cation but of different anions, the stability of the ionic liquids cannot be evaluated using LUMO values only without considering the molecular interaction energies.

To study the effect of cation on the reduction resistance of the ILs, the reduction potentials of 1,4-dibutyl-1,2,4-triazol-4-ium tetrafluoroborate (BBT BF_4) and 1-butyl-3-methylimidazolium tetrafluoroborate (BMIM BF_4) are compared as shown in Fig. 7. On the other hand, the computational HOMO/LUMO values of BBT and BMIM are shown in Fig. 8. Fig. 7 shows that BBT BF_4 has

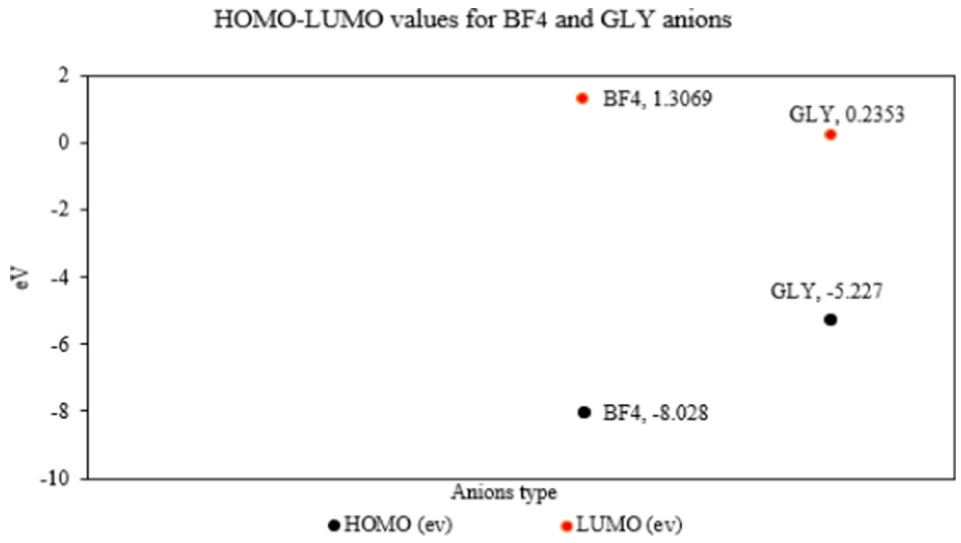

Fig. 6. HOMO-LUMO values for BF_4 and Glycine anions using Tmolex.

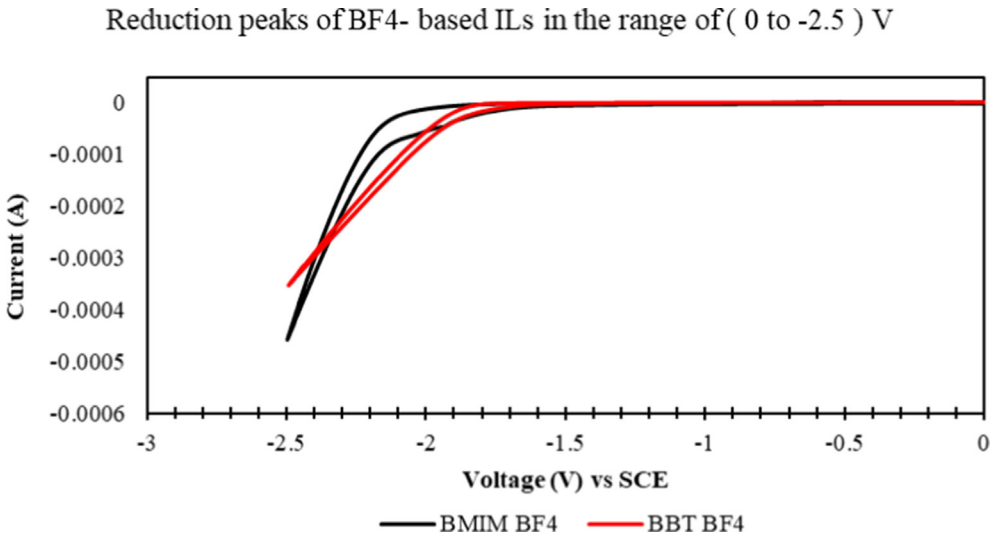

Fig. 7. Comparison between BBT BF_4 and BMIM BF_4 in terms of reduction peaks.

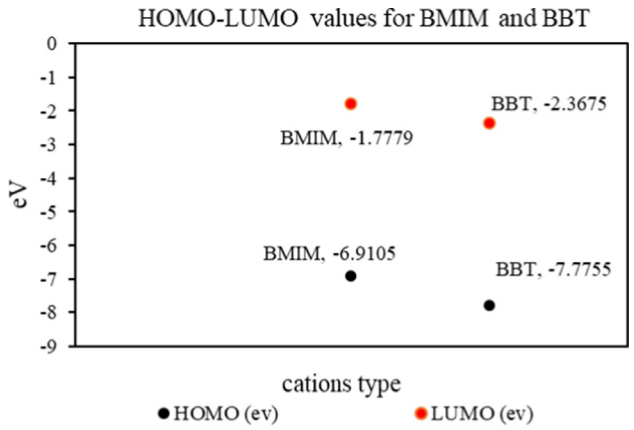

Fig. 8. HOMO-LUMO values for BMIM and BBT cations using Tmolex.

a slightly less reduction stability compared to BMIM BF_4. The reduction potential for BBT BF_4 is −1.65 V while it is −1.70 V for BMIM BF_4, which indicates that BBT BF_4 has a slightly lower LUMO value. A similar trend is observed in the computational study as shown in Fig. 8.

Another comparison between reduction peaks for 1-ethyl-3-methylimidazolium bis(trifluoromethylsulfonyl)imide (EMIM TFSI) and 1,4-dibutyl-1,2,4-triazol-4-ium bis(trifluoromethylsulfonyl)imide (BBT TFSI) is performed as shown in Fig. 9. From Fig. 9, it can be observed that BBT TFSI showed a lower reduction peak compared to EMIM TFSI. The reduction potential for BBT TFSI is −1.93 V while it is −2.22 V for EMIM TFSI, indicating that BBT has a lower LUMO value than EMIM. A similar trend is observed in the computational study in Fig. 10. The experiment shows that the reduction stability of ILs having the same anion but of different cations mainly depends on the LUMO values of the cations, since the cations are more exposed to the reduction's electrons due to the attraction force. Moreover, when comparing the cations, it

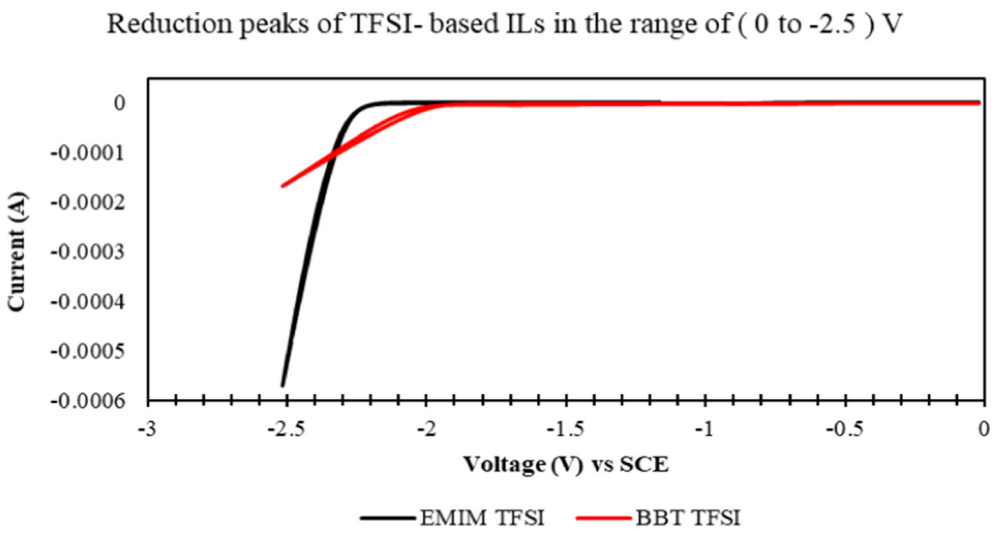

Fig. 9. Comparison between BBT TFSI and EMIM TFSI in terms of reduction peaks.

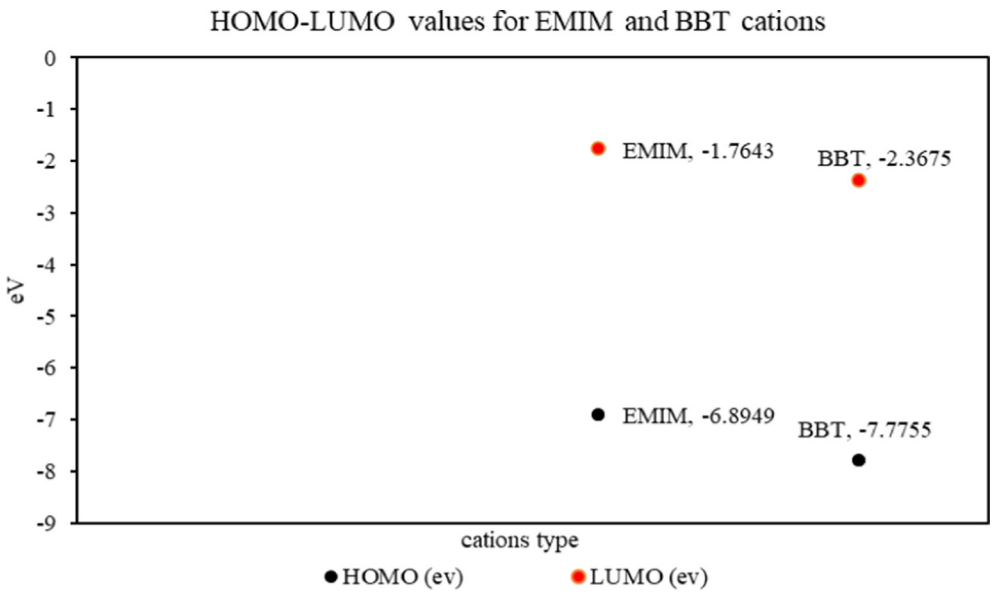

Fig. 10. HOMO-LUMO values for EMIM and BBT cations using Tmolex.

shows that the triazolium ILs are more easily reduced as compared to the imidazolium ILs. This can be explained by the presence of the additional electronegative nitrogen on the triazolium ring which introduces a small localized negative charge on the molecule as observed by the small red region in the COSMO-surface (*cf*. Fig. 4), thus lowering the LUMO values [57].

4. Conclusion

In conclusion, based on our experimental and computational studies of reduction potentials, the LUMO values of the ionic liquids are predominantly determined by the cation since it is closer to the reduction's electrons due to the attraction force. However, the effect of anions will influence the reduction potential in the case of a strong molecular interaction of the constituent ions. The strong repulsion force between the anion and the electrode enhances the stability of ILs toward the reduction. Moreover, the strong attraction force between the cation and anion stabilizes the reduction reaction since the anion behaves as a shield for the cation which increases the resistance towards reduction at the electrode. It can be concluded that for ILs having the same anion but of different cations, TmoleX software is useful to predict their reduction stability through the LUMO values of the cations. However, for the ILs having the same cation but of different anions, the reduction stability of the ionic liquid cannot be predicted using LUMO values only without considering the molecular interaction. This study will pave the way on targeting new types of stable ILs with relatively low LUMO values of cations and anions. Moreover, this study provides a perspective to enhance the use of computational method to predict the stability of ILs toward reduction.

CRediT authorship contribution statement

Sulafa Abdalmageed Saadaldeen Mohammed: Visualization, Investigation, Writing – original draft. **Wan Zaireen Nisa Yahya:** Conceptualization, Writing – review & editing, Supervision, Funding acquisition. **Mohamad Azmi Bustam:** Supervision, Resources. **Md Golam Kibria:** Supervision. **Asiah Nusaibah Masri:** Investiga-

tion, Validation. **Nurul Diyana Mohd Kamonwel:** Investigation, Validation.

Declaration of Competing Interest

The authors declare that they have no known competing financial interests or personal relationships that could have appeared to influence the work reported in this paper.

Acknowledgement

This research was funded by Fundamental Research Grant Scheme project from Ministry of Higher Education of Malaysia (FRGS/1/2021/TK0/UTP/02/12). The authors also acknowledge technical support and facilities from the Chemical Engineering Department and Centre of Research in Ionic Liquids of Universiti Teknologi PETRONAS.

Appendix A. Supplementary material

Supplementary data to this article can be found online at https://doi.org/10.1016/j.molliq.2022.119219.

References

[1] K. Matsumoto, J. Hwang, S. Kaushik, C.-Y. Chen, R. Hagiwara, Advances in sodium secondary batteries utilizing ionic liquid electrolytes, Energy Environ. Sci. 12 (11) (2019) 3247–3287.
[2] I. Osada, H. de Vries, B. Scrosati, S. Passerini, Ionic-liquid-based polymer electrolytes for battery applications, Angew. Chem. 55 (2) (2016) 500–513.
[3] C. Zhao, G. Burrell, A.A. Torriero, F. Separovic, N.F. Dunlop, D.R. MacFarlane, A. M. Bond, Electrochemistry of room temperature protic ionic liquids, J. Phys. Chem. B 112 (23) (2008) 6923–6936.
[4] N.a. Zhu, K. Zhang, F. Wu, Y. Bai, C. Wu, Ionic liquid-based electrolytes for aluminum/magnesium/sodium-ion batteries, Technology 2021 (2021) 1–29.
[5] W. Zhou, M. Zhang, X. Kong, W. Huang, Q. Zhang, Recent advance in ionic-liquid-based electrolytes for rechargeable metal-ion batteries, Adv. Sci. (2021) 2004490.
[6] N.I.M.F. Hilmy, W.Z.N. Yahya, K.A. Kurnia, Eutectic ionic liquids as potential electrolytes in dye-sensitized solar cells: physicochemical and conductivity studies, J. Mol. Liq. 320 (2020) 114381.
[7] P. Wang, L. Yang, H. Wu, Y. Cao, J. Zhang, N. Xu, S. Chen, J.D. Decoppet, S.M. Zakeeruddin, M. Grätzel, Stable and efficient organic dye-sensitized solar cell based on ionic liquid electrolyte, Joule 2 (10) (2018) 2145–2153.
[8] G. Bousrez, O. Renier, B. Adranno, V. Smetana, A.-V. Mudring, Engineering, "Ionic Liquid-Based Dye-Sensitized Solar Cells—Insights into Electrolyte and Redox Mediator Design,", ACS Sustain. Chem. Eng. 9 (24) (2021) 8107–8114.
[9] R. Atasiei, M. Raicopol, C. Andronescu, A. Hanganu, A.L. Alexe-Ionescu, G. Barbero, Investigation of the conduction properties of ionic liquid crystal electrolyte used in dye sensitized solar cells, J. Mol. Liq. 267 (2018) 81–88.
[10] R.A. Abu Talip, W.Z.N. Yahya, M.A. Bustam, Ionic liquids roles and perspectives in electrolyte for dye-sensitized solar cells, Sustainability 12 (18) (2020) 7598.
[11] J. Albo, M.I. Qadir, M. Samperi, J.A. Fernandes, I. de Pedro, J. Dupont, Use of an optofluidic microreactor and Cu nanoparticles synthesized in ionic liquid and embedded in TiO2 for an efficient photoreduction of CO_2 to methanol, Chem. Eng. J. 404 (2021) 126643.
[12] A. Atifi, D.W. Boyce, J.L. DiMeglio, J. Rosenthal, Directing the outcome of CO2 reduction at bismuth cathodes using varied ionic liquid promoters, ACS Catal. 8 (4) (2018) 2857–2863.
[13] M. Zeng, Y. Liu, Y. Hu, X. Zhang, High-efficient CO_2 electrocatalysis over nanoporous Au film enabled by a combined pore engineering and ionic liquid-mediated approach, Chem. Eng. J 425 (2021) 131663.
[14] W. Lu, B. Jia, B. Cui, Y. Zhang, K. Yao, Y. Zhao, J. Wang, Efficient photoelectrochemical reduction of carbon dioxide to formic acid: a functionalized ionic liquid as an absorbent and electrolyte, Angew. Chem. Int. Ed. 56 (2017) 11851–11854.
[15] K. Fic, B. Gorska, P. Bujewska, F. Béguin, E. Frackowiak, Selenocyanate-based ionic liquid as redox-active electrolyte for hybrid electrochemical capacitors, Electrochim. Acta 314 (2019) 1–8.
[16] B. Gorska, L. Timperman, M. Anouti, F. Béguin, Effect of low water content in protic ionic liquid on ions electrosorption in porous carbon: application to electrochemical capacitors, Phys. Chem. Chem. Phys. 19 (18) (2017) 11173–11186.
[17] M.C. Santos, G.G. Silva, R. Santamaría, P.F. Ortega, R.L. Lavall, Discussion on operational voltage and efficiencies of ionic-liquid-based electrochemical capacitors, J. Phys. Chem. C 123 (14) (2019) 8541–8549.
[18] E.P. Yambou, B. Gorska, F. Béguin, Electrical double-layer capacitors based on a ternary ionic liquid electrolyte operating at low temperature with realistic gravimetric and volumetric energy outputs, ChemSusChem 14 (4) (2021) 1196–1208.
[19] J. Lohrman, C. Zhang, W. Zhang, S. Ren, Semiconducting carbon nanotube and covalent organic polyhedron–C 60 nanohybrids for light harvesting, Chem. Commun. 48 (67) (2012) 8377–8379.
[20] M. Galiński, A. Lewandowski, I. Stepniak, Ionic liquids as electrolytes, Electrochim. Acta 51 (2006) 5567–5580.
[21] D. Chen, J. Cheng, Y. Wen, G. Cao, Y. Yang, H. Liu, Impedance study of electrochemical stability limits for electrolytes, Int. J. Electrochem. Sci 7 (2012) 12383–12390.
[22] S. Murugesan, O.A. Quintero, P.B. Chou, P. Xiao, K. Park, J.W. Hall, R.A. Jones, G. Henkelman, J.B. Goodenough, K.J. Stevenson, Wide electrochemical window ionic salt for use in electropositive metal electrodeposition and solid state Li-ion batteries, J. Mater. Chem. A 2 (7) (2014) 2194–2201.
[23] S.P. Ong, O. Andreussi, Y. Wu, N. Marzari, G. Ceder, Electrochemical windows of room-temperature ionic liquids from molecular dynamics and density functional theory calculations, Chem. Mater. 23 (11) (2011) 2979–2986.
[24] Y. Zhang, C. Shi, J.F. Brennecke, E. Maginn, Refined method for predicting electrochemical windows of ionic liquids and experimental validation studies, J. Phys. Chem. B 118 (23) (2014) 6250–6255.
[25] N.V. Ilawe, J. Fu, S. Ramanathan, B.M. Wong, J. Wu, Chemical and radiation stability of ionic liquids: a computational screening study, J. Phys. Chem. C 120 (49) (2016) 27757–27767.
[26] L. Maftoon-Azad, Electrochemical stability windows of Ali-cyclic ionic liquids as lithium metal battery Electrolytes: a computational approach, J. Mol. Liq. 343 (2021) 117589.
[27] A. Paolone, S. Brutti, Comparison of the performances of different computational methods to calculate the electrochemical stability of selected ionic liquids, Materials 14 (12) (2021) 3221.
[28] T.C. Lourenço, L.G. Dias, J.L. Da Silva, Theoretical investigation of the Na+ transport mechanism and the performance of ionic liquid-based electrolytes in sodium-ion batteries, ACS Appl. Energy Mater. 4 (5) (2021) 4444–4458.
[29] F. Chen, M. Forsyth, Computational investigation of mixed anion effect on lithium coordination and transport in salt concentrated ionic liquid electrolytes, J. Phys. Chem. Lett. 10 (23) (2019) 7414–7420.
[30] S. Kazemiabnavi, Z. Zhang, K. Thornton, S. Banerjee, Electrochemical stability window of imidazolium-based ionic liquids as electrolytes for lithium batteries, J. Phys. Chem. B 120 (25) (2016) 5691–5702.
[31] R. Hagiwara, Y. Ito, Room temperature ionic liquids of alkylimidazolium cations and fluoroanions, J. Fluor. Chem. 105 (2) (2000) 221–227.
[32] S. Asha, K.P. Vijayalakshmi, B.K. George, Pyrrolidinium-based ionic liquids as electrolytes for lithium batteries: a Computational Study, Int. J. Quantum Chem. 119 (22) (2019), https://doi.org/10.1002/qua.v119.2210.1002/qua.26014.
[33] M. Hayyan, F.S. Mjalli, M.A. Hashim, I.M. AlNashef, T.X. Mei, Investigating the electrochemical windows of ionic liquids, J. Ind. Eng. Chem. 19 (1) (2013) 106–112.
[34] P.C. Howlett, E.I. Izgorodina, M. Forsyth, D.R. MacFarlane, Electrochemistry at negative potentials in bis (trifluoromethanesulfonyl) amide ionic liquids, Z. Phys. Chem 220 (10) (2006) 1483–1498.
[35] S.S. Manna, P. Bhauriyal, B. Pathak, Identifying suitable ionic liquid electrolytes for Al dual-ion batteries: role of electrochemical window, conductivity and voltage, Mater. Adv. 1 (5) (2020) 1354–1363.
[36] P. Peljo, H.H. Girault, Electrochemical potential window of battery electrolytes: the HOMO–LUMO misconception, Energy Environ. Sci. 11 (9) (2018) 2306–2309.
[37] Q. Li, J. Jiang, G. Li, W. Zhao, X. Zhao, T. Mu, The electrochemical stability of ionic liquids and deep eutectic solvents, Sci. China Chem. 59 (5) (2016) 571–577.
[38] T.L. Greaves, A. Weerawardena, C. Fong, I. Krodkiewska, C. Drummond, Protic ionic liquids: solvents with tunable phase behavior and physicochemical properties, J. Phys. Chem. B 110 (45) (2006) 22479–22487.
[39] Z. Xue, L. Qin, J. Jiang, T. Mu, G. Gao, Thermal, electrochemical and radiolytic stabilities of ionic liquids, Phys. Chem. Chem. Phys. 20 (13) (2018) 8382–8402.
[40] S.A.S. Mohammed, W.Z.N. Yahya, M.A. Bustam, A. Nzihou, R. Boopathy, M. Nasef, S. Yusup, D.C.W. Tsang, N.A. Amran, B. Abdullah, Computational studies of ionic liquids as co-catalyst for CO_2 electrochemical reduction to produce syngas using COSMO-RS, E3S Web of Conf. 287 (2021) 02016, https://doi.org/10.1051/e3sconf/202128702016.
[41] S.A.S. Mohammed, W.Z.N. Yahya, M.A. Bustam, M.G. Kibria, Elucidation of the roles of ionic liquid in CO_2 electrochemical reduction to value-added chemicals and fuels, Molecules 26 (22) (2021) 6962.
[42] C. Steffen, K. Thomas, U. Huniar, A. Hellweg, O. Rubner, A. Schroer, TmoleX—a graphical user interface for TURBOMOLE, J. Comput. Chem. 31 (16) (2010) 2967–2970.
[43] A. Klamt, COSMO-RS for aqueous solvation and interfaces, Fluid Ph. Equilibria 407 (2016) 152–158.
[44] S. Balchandani, R. Singh, Thermodynamic analysis using COSMO-RS studies of reversible ionic liquid 3-aminopropyl triethoxysilane blended with amine activators for CO_2 absorption, J. Mol. Liq. 324 (2021) 114713.
[45] C.Y. Foong et al., COSMO-RS prediction and experimental investigation of amino acid ionic liquid-based deep eutectic solvents for copper removal, J. Mol. Liq. 333 (2021) 115884.
[46] H.W. Khan, A.A.M. Elgharbawy, A. Bustam, M. Moniruzzaman, Design and Selection of Ionic Liquids Via COSMO for Pharmaceuticals and Medicine, in: M. Goto, M. Moniruzzaman (Eds.), Application of Ionic Liquids in Drug Delivery,

Springer Singapore, Singapore, pp. 137–164, https://doi.org/10.1007/978-981-16-4365-1_8.
[47] M.R. Atkinson, J.B. Polya, Triazoles. Part II. N-substitution of some 1 : 2 : 4-triazoles, J. Chem. Soc. (1954) 141, https://doi.org/10.1039/jr9540000141.
[48] J.L. Belletire, R.A. Bills, S.A. Shackelford, Practical methylation procedure for (1H)-1, 2, 4-Triazole, Synth. Commun. 38 (5) (2008) 738–745.
[49] A. Klamt, Conductor-like screening model for real solvents: a new approach to the quantitative calculation of solvation phenomena, J. Phys. Chem. 99 (7) (1995) 2224–2235.
[50] A. Klamt, V. Jonas, T. Bürger, J.C. Lohrenz, Refinement and parametrization of COSMO-RS, J. Phys. Chem A 102 (26) (1998) 5074–5085.
[51] M. Shyama, S. Lakshmipathi, Cation-anion interactions, stability, and IR spectra of dicationic amino acid-based ionic liquids probed using density functional theory, J. Mol. Model. 27 (6) (2021) 1–12.
[52] E. Thomas, K.P. Vijayalakshmi, B.K. George, Kinetic stability of imidazolium cations and ionic liquids: a frontier molecular orbital approach, J. Mol. Liq. 276 (2019) 721–727.
[53] J. Li, X. Yang, K. Chen, Y. Zheng, C. Peng, H. Liu, Sifting ionic liquids as additives for separation of acetonitrile and water azeotropic mixture using the COSMO-RS method, Ind. Eng. Chem. Res 51 (27) (2012) 9376–9385.
[54] C. Loschen, A. Klamt, Prediction of solubilities and partition coefficients in polymers using COSMO-RS, Ind. Eng. Chem. Res 53 (28) (2014) 11478–11487.
[55] K. Chatterjee, A.D. Pathak, A. Lakma, C.S. Sharma, K.K. Sahu, A.K. Singh, Synthesis, characterization and application of a non-flammable dicationic ionic liquid in lithium-ion battery as electrolyte additive, Sci. Rep. 10 (1) (2020) 1–12.
[56] H. Zhang, H. Zhao, M.A. Khan, W. Zou, J. Xu, L. Zhang, J. Zhang, Recent progress in advanced electrode materials, separators and electrolytes for lithium batteries, J. Mater. Chem. A 6 (42) (2018) 20564–20620.
[57] M. Idris, C. Coburn, T. Fleetham, J. Milam-Guerrero, P.I. Djurovich, S.R. Forrest, M.E. Thompson, Phenanthro [9, 10-d] triazole and imidazole derivatives: high triplet energy host materials for blue phosphorescent organic light emitting devices, Mater. Horiz. 6 (6) (2019) 1179–1186.